

The Moisture-Entrainment-Convection Feedback Can Lead to Spontaneous Tropical Cyclone Genesis

Argel Ramírez Reyes* (1) and Da Yang* (1, 2)

Affiliations:

1. University of California, Davis
2. Lawrence Berkeley National Laboratory

*Contact information:

aramirezreyes@ucdavis.edu

dayang@ucdavis.edu

Key points:

1. Spontaneous TC genesis can occur without radiative and surface flux feedbacks.
2. The moisture-entrainment-convection feedback can lead to spontaneous TC genesis and intensification.
3. The moisture-entrainment-convection feedback can operate in a time scale of a few hours, efficient to influence TC genesis in the real world.

Abstract

In contrast to prevailing knowledge, Ramírez Reyes and Yang (2021) showed that tropical cyclones (TCs) can form spontaneously without moisture-radiation and surface-flux feedbacks in a cloud-resolving model (CRM) simulation. Here we ask, why? Fourteen 3D cloud-resolving simulations show that the moisture-entrainment-convection (MEC) feedback can effectively lead to spontaneous TC genesis and intensification in the absence of radiative and surface-flux feedbacks. In the MEC feedback, a moister environment favors new deep convective events that further moisten the environment, leading to aggregation of deep convection. The impact of the MEC feedback on TC genesis and intensification occurs in two distinct time scales: a short time scale set by detrainment moistening the environment (a few hours) and a long time scale (17 days) due to subsidence drying. The hours-long time scale of detrainment suggests that the MEC feedback is an efficient process relevant to TC genesis in the real world.

Plain language summary

Computer simulations show that dispersed thunderstorms tend to self-organize into a tropical cyclone (TC). This process occurs even in highly idealized climates without the most common processes that, in nature, are observed to aid TC formation (e.g., pre-existing disturbance or special structure in ocean energy fluxes and radiative energy fluxes). What causes tropical cyclones to form in such an exotic atmosphere? We find, using computer simulations, that thunderstorms and environmental moisture reinforce one another, causing disorganized patches of storms to aggregate into a tropical cyclone. We call this the moisture-entrainment-convection (MEC) feedback. By varying our simulation parameters, we find that the MEC feedback operates over periods of a few hours to several weeks. The fast (hours-long) component of the MEC feedback may be important for understanding and forecasting the genesis of real-world TCs.

1. Introduction

In Earth's atmosphere, there are around 90 tropical cyclones (TCs) every year. They are warm-core, rapidly rotating storms with horizontal scales of the order of 500 km in maturity and are typically formed over tropical oceans. Despite extensive research and improved forecast

techniques, uncertainties in forecasting TC genesis and intensification hinder safety and evacuation planning by policymakers. TC-associated intense rainfall, strong winds, and storm surge continue to cost lives, economic losses, and societal impacts. Therefore, improving our understanding of TC genesis and intensification is of primary importance in tropical meteorology and atmospheric science.

In computer simulations, TCs can self-emerge from random convection over uniform sea-surface temperatures on an f -plane (Bretherton et al., 2005; Carstens & Wing, 2020; Davis, 2015). This phenomenon is known as *spontaneous TC genesis* and offers a simplified framework to understand TC genesis without the full complexity of the real atmosphere. Wing et al. (2016) showed that spontaneous TC genesis requires either radiative feedback or surface-flux feedback. This result was then confirmed and recast by Muller and Romps (2018) using small-domain (1000 km x 1000 km) cloud-resolving simulations. However, Ramírez Reyes and Yang (2021) showed that TCs can self-emerge without radiative and surface flux feedbacks using the same cloud-resolving model (CRM). A major difference is that Ramírez Reyes and Yang (2021) used a higher Coriolis parameter, making TCs smaller and easier to fit into a limited computing domain. This result challenges the prevailing understanding of spontaneous TC genesis.

What leads to spontaneous TC genesis and intensification without radiative and surface flux feedbacks? Here, we test the hypothesis that the moisture-entrainment-convection (MEC) feedback leads to TC genesis and intensification in the study of Ramírez Reyes and Yang (2021). In the MEC feedback, moisture detrained from deep convection promotes new convective events in the same region, leading to the organization of convection. Organized convection could help TC genesis by moistening the lower troposphere and maintaining a moist adiabat, which inhibits evaporation of rain and its associated divergence in the low levels (D.S. Nolan, 2007; Raymond et al., 2007; Wang, 2012). The MEC feedback was first proposed by Scorer and Ludlam (1953) and it recently gained relevance from the thorough studies of Tompkins (2001). Since then, several authors have studied the impact of the MEC feedback in organizing convection (G. C. Craig & Mack, 2013; Grabowski & Moncrieff, 2004; Kuang & Bretherton, 2006; Seeley & Romps, 2015; Tompkins & Semie, 2017; Wang, 2014; Yang, 2019).

In this work, we use high-resolution simulations to test the hypothesis that the MEC feedback is responsible for spontaneous TC genesis and intensification without radiative and surface-flux feedbacks in the simulations of Ramírez Reyes and Yang (2021). We also explore the time scales in which the components of this feedback operate, and we discuss if the MEC feedback could be relevant to real TC genesis.

2. Hypothesis: the MEC feedback leads to spontaneous TC genesis in the absence of radiative and surface-flux feedbacks

2.1 The Moisture-Entrainment-Convection feedback

Figure 1 illustrates the main ingredients of the MEC feedback. A deep convective cloud with vertical velocity W_c exchanges mass with the environment through turbulent detrainment and entrainment, with fractional detrainment and entrainment rates of δ and ϵ , respectively. In the clear-sky environment, air subsides with a characteristic vertical wind speed of W_s .

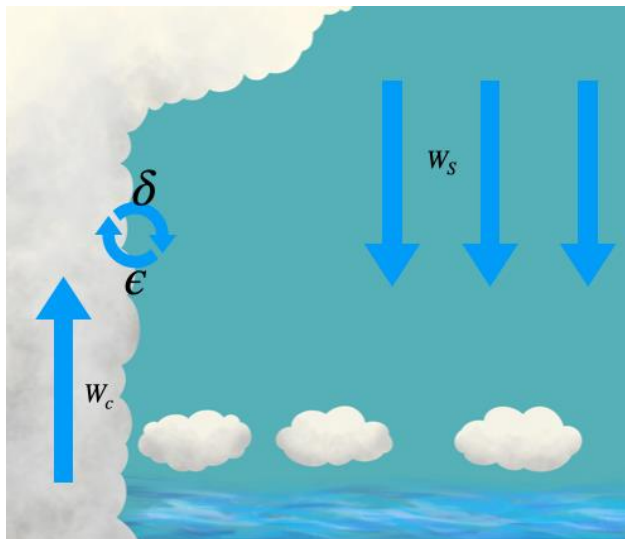


Figure 1. Illustration of the characteristic lengths and velocities of convection that set the time scales τ_d and τ_s .

Dry environments inhibit deep convection, and moist environments favor deep convection. Mixing of environmental air into convective updrafts reduces the buoyancy of the convecting parcels due to evaporative cooling (Tompkins & Semie, 2017) and to the buoyancy effect of water vapor

(Seidel & Yang, 2020; Yang & Seidel, 2020). This implies that the mixing of moist environmental air into the updrafts results in a smaller buoyancy reduction than it would if the environment were drier. Reciprocally, moist convection influences moisture in the environment. Detrainment from convective clouds into the environment creates an anomalously moist region that favors new deep convective events in the vicinity of existing convective clouds and around the location of recently extinct convective clouds. In clear-sky regions, subsidence dries the atmosphere, inhibiting new deep convective events. This reciprocal interaction of environmental moisture and convection constitutes a feedback process that promotes the organization of deep convection. To the best of our knowledge, this feedback was first proposed by Scorer and Ludlam (1953) and discussed by Randall and Huffman (1980). It has been thoroughly examined by Tompkins (2001) in studies of convective self-aggregation; this feedback was then further developed and applied to study the convective organization of the tropical atmosphere (G. C. Craig & Mack, 2013; Grabowski & Moncrieff, 2004; Kuang & Bretherton, 2006; Seeley & Romps, 2015; Yang, 2019) and by Wang (2014) in the study of TC genesis in numerical models. Below we analyze two characteristic timescales associated with this feedback; both timescales contribute to the generation of horizontal moisture gradients.

2.2 Entrainment and detrainment timescale

The cloudy air ascending at vertical velocity W_c will exchange mass with the environment with a fractional detrainment rate δ (with units of $1/m$). This entrainment rate corresponds to a length $\text{Length}_\delta \equiv \frac{1}{\delta}$ over which convection moistens the environment. A typical value of the fractional detrainment rate of deep convection on Earth is 0.2 km^{-1} (Romps, 2014). Using a characteristic vertical velocity of the convecting plume of 1 ms^{-1} (close to the median vertical velocity of updrafts in some observations of tropical deep convection (Lucas et al., 1994)), we find that the moistening time scale is

$$\tau_d = \frac{\text{Length}_\delta}{W_c} \approx \frac{5000 \text{ m}}{1 \text{ ms}^{-1}} \approx 1.38 \text{ hours.}$$

Here we assume that, in the leading order, the entrainment and detrainment rates are approximately equal (Romps, 2014).

2.3 Subsidence timescale

In clear-sky regions, air subsides with a characteristic velocity W_s , which in the outer region of a TC has values around 2 mm s^{-1} (Chavas et al., 2015). A characteristic length of the problem is the scale height of water vapor which has values around 3000 m (Romps, 2014). With these two ingredients, we can estimate the time scale of drying by subsidence:

$$\tau_s = \frac{\text{Water vapor scale height}}{W_s} \approx \frac{3000 \text{ m}}{0.002 \text{ m s}^{-1}} \approx 17 \text{ days.}$$

We note that τ_s is much longer than τ_d , suggesting detrainment of water vapor is a more efficient process in creating horizontal moisture perturbations.

2.4 Expectations

We hypothesize that the MEC feedback is responsible for spontaneous TC genesis in the absence of a pre-existing disturbance or other feedbacks that promote the organization of deep convection. This hypothesis makes two predictions: P1) A decrease of entrainment into and detrainment from clouds will inhibit spontaneous TC genesis, and P2) homogenization of clear-sky water vapor on a *shorter* time scale than τ_d will effectively remove horizontal water vapor gradients and will thereby inhibit spontaneous TC genesis.

Additionally, subsidence of dry air inhibits convection outside the core of a TC with a time scale of τ_s . Inhibiting convection outside the core allows convection to be concentrated near the core, favoring the intensification of TCs. Therefore, we expect that moistening the descending branch on a time scale faster than τ_s will prevent the intensification of the spontaneously formed TCs (P3).

3. Methods

3.1 The cloud-permitting model and simulation details

We run 3D simulations using the *System for atmospheric modeling* (SAM, version 6.10.10) (Khairoutdinov & Randall, 2003). SAM solves the anelastic equations of motion using a finite-difference numerical scheme in an Arakawa-C grid. Regarding thermodynamics, SAM solves the conservation equation for frozen moist static energy. We use the CAM radiation scheme for long-wave and short-wave fluxes (Collins et al., 2004), and the default SAM single-moment bulk microphysics scheme. The latent and sensible heat fluxes are computed using a bulk formulation

where the transfer coefficients are computed using the Monin-Obukhov theory with code adapted from the Community Climate Model 3 (Kiehl et al., 1996). We used the SAM Smagorinsky SGS parameterization described in (Deardorff, 1980). SAM does not employ a specific parameterization for the boundary layer. We output 3D fields every two hours and 2D fields every hour.

The simulation domain is a square of 1024 km x 1024 km in the horizontal dimensions and 34.8 km in the vertical. Grid spacing is 2 km in the horizontal, and in the vertical, it is 50 m from $z = 0$ m to $z = 1050$ m. Then, the vertical grid spacing increases gradually until $z = 3000$ m, where it becomes 600 m. The boundary conditions are periodic in the horizontal directions. The bottom boundary is an ocean with a fixed surface temperature of 300 K, and the upper 30 levels are a sponge layer to prevent the reflection of gravity waves. We use a constant Coriolis parameter of $f = 5 \times 10^{-4} \text{ s}^{-1}$. This value is ten times that of 20° latitude on Earth. A similar value has been used before (Cronin & Chavas, 2019; Khairoutdinov & Emanuel, 2013; Ramírez Reyes & Yang, 2021). The increased Coriolis parameter is necessary for spontaneous TC genesis without radiative and surface flux feedbacks in this domain and with a grid spacing of 2 km (Ramírez Reyes & Yang, 2021), and it also allows for the reduction of the size of individual TCs, allowing several TCs to exist in this domain (Khairoutdinov & Emanuel, 2013). While in real Earth, radiative and surface-flux feedbacks may be necessary for TC genesis to occur, turning them off allows us to explore in detail the role of the MEC feedback. The knowledge gained from this framework can then be compared to more realistic simulations. We initialize the simulations using a sounding from the last days of a non-rotating RCE simulation, the same profile used in (Yang, 2018). In all the simulations, we disable the radiative and surface-flux feedbacks by substituting surface heat fluxes and radiative fluxes by their horizontally averaged value before applying them (Muller & Romps, 2018; Ramírez Reyes & Yang, 2021; Wing et al., 2016).

3.2 Experiment design: Weakening the MEC feedback

We design experiments to test P1–P3 by reducing entrainment and detrainment rates and by homogenizing clear-sky water vapor. We run in total 14 simulations. Our Control simulation is similar to the HomoAll experiment of Ramírez Reyes and Yang (2021), where radiative and surface-flux feedbacks are disabled by substituting radiative heating rate and surface fluxes with

their horizontal averages before applying them (Muller & Romps, 2018; Ramírez Reyes & Yang, 2021; Wing et al., 2016). Although we expect the buoyancy effect of water vapor on buoyancy of the convecting cloud to be small when compared to the effects of energy released by phase changes (Yang, 2018), we turn off the buoyancy effect of water vapor as in (Yang, 2019) to further simplify the system. We then perform the following experiments:

i. Disabling the MEC feedback by turning off SGS mixing:

This experiment consists of one run that differs from Control only by turning off the mixing of water vapor fields from the SGS parameterization. This simulation will be referred to as NoSGS. In this study, we use a grid spacing of 2 km. At this resolution, a significant part of the entrainment and detrainment from clouds still depends on the SGS parameterization (Bryan et al., 2003; George C. Craig & Dörnbrack, 2008; Tompkins & Semie, 2017). By turning off the SGS parameterization we remove the unresolved portion of entrainment and detrainment, allowing us to directly test P1.

ii. Weakening the MEC feedback by homogenizing clear-sky water vapor

This experiment consists of a set of simulations that differ from Control by relaxing (nudging) the clear-sky (unsaturated grid points) water vapor toward its horizontal average. In the anomalously moist regions, homogenizing clear-sky water vapor means drying; in the anomalously dry regions, it is moistening. To homogenize clear-sky water vapor, we add a relaxation term to the water vapor field in the unsaturated grid points as done by Yang (2019).

$$\widetilde{\delta r}(i, j, k, t_i) \Delta t = \begin{cases} \delta r(i, j, k, t_i) \Delta t & \text{if } r_{cond}(i, j, k, t_i) > 0.01 \text{ g kg}^{-1} \\ \delta r(i, j, k, t_i) \Delta t + (\bar{r}(k, t_i) - r(i, j, k, t_i)) \Delta t / \tau_r & \text{otherwise} \end{cases} ,$$

where $i, j, and k$ represent the grid indices in the space dimensions and t_i represents the time index. δr is the original tendency of the water vapor field computed by SAM and multiplied by the timestep Δt . r_{cond} is the total condensate mixing ratio. The overbar represents an average over all the points that fulfill the same criterion of low condensate. τ_r is the relaxation time scale. We let τ_r take 12 values between 0.5 h and 15 days (see Table 1). This method resembles the relaxation done by Seeley and Romps (2015), except that they nudged the relative humidity field. Similar to the method employed by Seeley and Romps, our method effectively reduces moisture gradients (Figure 1).

| Name | Differences from the Control experiment | Grid size | Domain size | Simulation length | Number of simulations |
|---------|---|------------|-----------------------------|-------------------|-----------------------|
| Control | None | 512x512x80 | 1000 km x 1000 km x 34.8 km | 100 days | 1 |
| NoSGS | Disable SGS parameterization | 512x512x80 | 1000 km x 1000 km x 34.8 km | 100 days | 1 |
| Nudging | Out-of-cloud water vapor nudged to horizontal mixing ratio of out-of-cloud water vapor with timescales: 0.5h, 1h, 2h, 3h, 5h, 8h, 12h, 1d, 2d, 5d, 10d, 15d | 512x512x80 | 1000 km x 1000 km x 34.8 km | 100 days | 12 |

Table 1. Summary of simulation parameters in the mechanism-denial experiments.

3.3 Detection and characterization of TC-associated inflow and updrafts

To characterize the location of convective updrafts relative to the TC centers and the intensity of the inflow we first identify TC centers as local minima of surface pressure at each time step during each 10-day period of each simulation. Next, we compute the total number of updrafts (defined as grid points where the vertical velocity exceeds 2 ms^{-1}) that occur at each distance from the center (using 2-km bins starting in $r = 1 \text{ km}$) and divide it by the number of points that fall within said bin (a measure of the area of the region that falls between said bins). Finally, we divide the total number of updrafts that occur between $r = 3r_{max}$ and $r = 6r_{max}$ by those that appear between $r = 0$ and $r = 6r_{max}$. This quantity, which we call the “updraft ratio” shows how concentrated convection is near the radius of maximum winds. TCs that have the most convective events near the radius of maximum winds would have an updraft ratio close to zero, and TCs that have as many updrafts close to the radius of maximum winds as far from it would have an updraft ratio close to 0.5. To compute the inflow we create an “average” TC by aligning each center and averaging the

velocity fields, as in (Ramírez Reyes & Yang, 2021). We then compute the mean radial velocity in a region bounded by the radius of maximum winds (r_{max}) and $6r_{max}$ in the radial direction, and from the surface to 6 km height. We perform the calculation for all the experiments with TCs for 10-day periods between day 60 and 100 (e.g., day 60 to 70, 70 to 80, 80 to 90 and 90 to 100).

4. Results

Removal of turbulent entrainment and detrainment of water vapor from clouds removes spontaneous TC genesis (P1). Figure 2 shows a snapshot of surface wind speed at day 95 of the Control and NoSGS simulations. In Control we observe well-formed TCs with maximum wind speeds of around 40 m s^{-1} around a region of quiescent winds (their eye). In NoSGS, no TCs develop, and instead, regions of high speed (wind gusts) and low speed are equally distributed throughout the domain. The uniform distribution of convective and non-convecting patches supports that the mixing of cloudy and non-cloudy air is a necessary ingredient for spontaneous TC genesis and for the emergence of any organization of convection.

Homogenizing clear-sky water vapor on a timescale shorter than τ_d prevents spontaneous TC genesis (P2). TCs spontaneously emerge in Control and in simulations with nudging timescale τ_r between 2 hours and 15 days. However, no TCs form in simulations with nudging timescales smaller than 2 hours. In Figure 2 we show snapshots of precipitable water (PW), surface wind speed, and surface pressure at day 95 for a selected subset of simulations (see also Movie S1). We observe that the PW shows negligible spatial variance for the short relaxation time scales (e.g., $\tau_r = 0.5$ hours or $\tau_r = 1$ hour), which increases as τ_r becomes longer. In Control and $\tau_r = 15$ days, there are distinct large-scale high PW regions that coincide with the TCs, which is surrounded by low PW regions. For relaxation time scales below 2 hours, we observe randomly distributed winds with maximum speeds of around 10 m s^{-1} . When τ_r increases above 2 hours, we observe regions of increased surface wind speed around the eye. TCs in the experiments with τ_r between 3 hours and 5 days show modest intensities by day 60, while experiments with relaxation time scales above 10 days show similar intensities to TCs in Control.

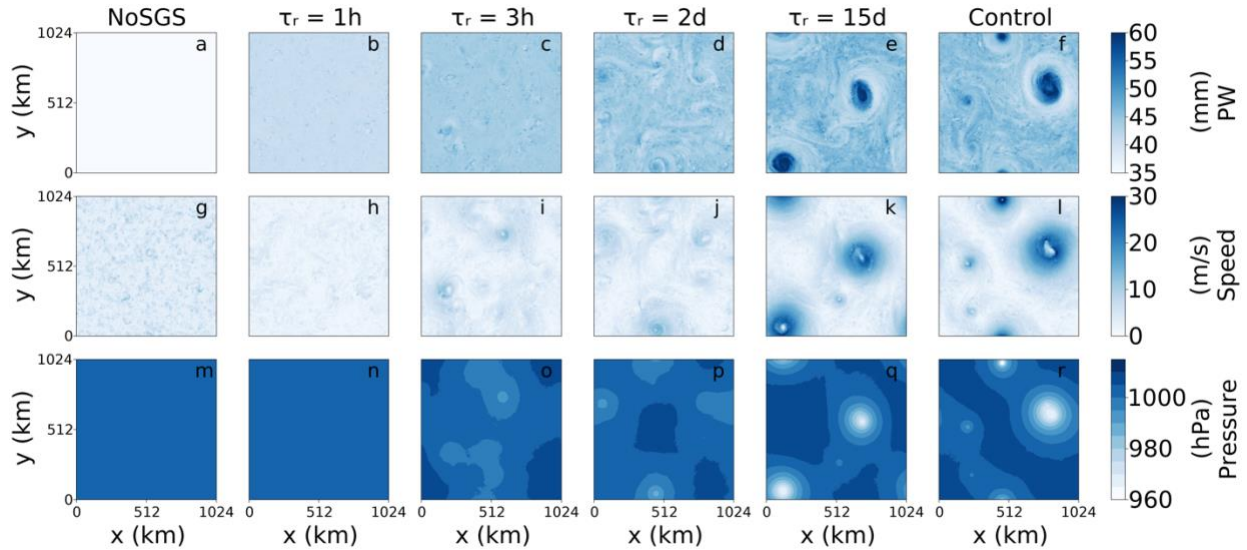


Figure 2. Map views of precipitable water, surface pressure, and surface wind speed at $t = 95$ days (snapshot). (a-f) precipitable water (mm), (g-l) surface wind speed (m s^{-1}), and (m-r) surface pressure (hPa). The first column corresponds to NoSGS, columns 2-5 correspond to experiments with water vapor relaxation time scales of 1 h, 3 h, 2 days, and 15 days respectively, and the sixth column is the Control experiment. Simulations with 2-km grid spacing.

Our experiments also support P3 and show that homogenizing clear-sky water vapor on a multi-day time scale prevents the intensification of spontaneously formed TCs. The behavior of simulations can be described as three distinct regimes: No TCs, weak TCs, and intense TCs (similar in intensity to those in Control). Figure 3 shows maximum surface wind speed and minimum surface pressure in the domain versus time for a selected subset of experiments (see Figure S2 for all the experiments). The experiments with τ_r below 2 hours show almost constant maximum wind speeds of around 15 ms^{-1} (corresponding to random wind gusts) and nearly constant minimum surface pressures of around 1000 hPa. These simulations show random convection. Experiments with τ_r higher than 2 hours show stronger wind speeds and lower pressures at the surface: after an initial intensification period, simulations with τ_r between 3 hours and 5 days show surface wind speeds and surface pressures fields that oscillate around 20 ms^{-1} and 990 hPa, corresponding to weak TCs. Finally, the experiment with τ_r equal to 15 days mimics the Control simulation, with maximum wind speeds oscillating around 40 ms^{-1} and minimum

surface pressures that oscillate around 960 hPa after an intensification period. These three regimes (“short” relaxation time scales with no organization, “moderate” relaxation time scales with weak TCs and “long” relaxation time scales with strong TCs) suggest that the coupling between environmental water vapor and convection may operate in two different mechanisms in TC genesis and TC intensification. A fast process is instrumental for initial convective organization and spontaneous TC genesis, and a slower process helps TC intensification. These results are consistent with P3. We note though, that the simulations with $\tau_r = 5$ days and $\tau_r = 10$ days reach similar intensities to Control by the end of the 100-day period (Figure S1). This suggests that the transition between the no non-intensifying and the intensifying regime may not be abrupt. A more detailed study of the transition would require substantial increase in computational and is left to future work.

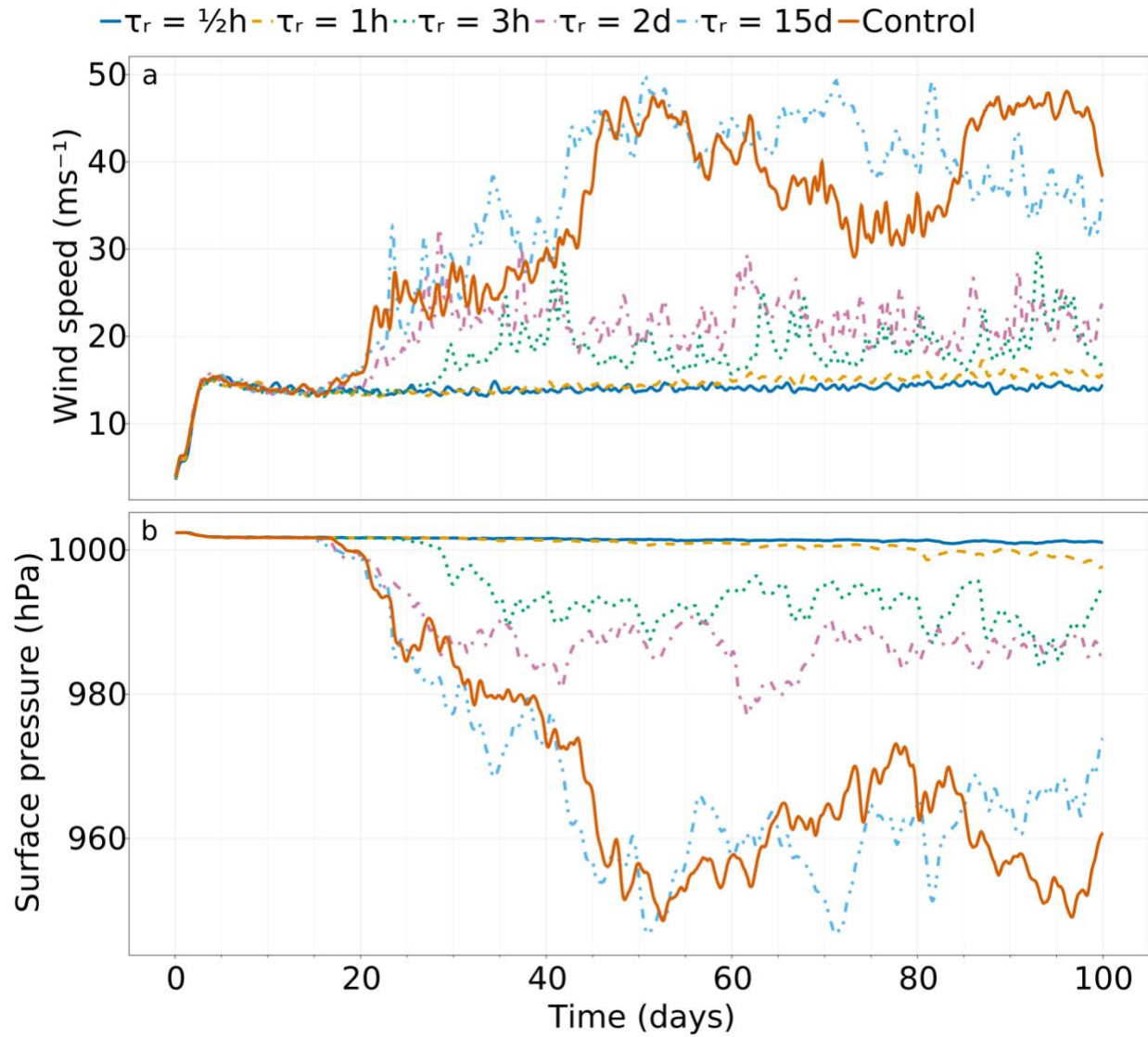


Figure 3. Time evolution of maximum surface wind speed (m/s) (a) and minimum surface (hPa) (b). Hourly data is smoothed with a moving average filter with window = 12 hours.

Here we speculate about how clear-sky water vapor homogenization on a multi-day time scale prevents the intensification of TCs. Intensification of TCs requires strong inflow to bring air parcels closer to the eyewall while nearly maintaining their angular momentum. This amplifies the tangential wind speeds and intensifies the TC (Montgomery & Smith, 2014). Meanwhile, drying by subsidence beyond the eyewall opposes the appearance of convection beyond the TC eyewall. In our experiments, homogenizing water vapor leads to moistening of the subsiding areas, allowing

deep convective events beyond the radius of the eyewall. This increased convection beyond the eyewall reduces the inflow to the eyewall and therefore opposes the intensification of the TCs.

To test this hypothesis, Figure 4 shows the relationship between mean inflow and updraft ratio, which measures how concentrated updrafts are near the radius of maximum tangential winds (a value close to 0.0 shows that convection is concentrated and a value of 0.5 shows that convection is uniformly distributed). In our experiments, the updraft ratio is related to the mean inflow approximately by $\log(\text{inflow}) = -2.77 * \text{updraft ratio}$ (correlation coefficient = -0.77), showing that TCs with most updrafts concentrated near r_{max} have a stronger inflow than those where convection is uniformly distributed at all radii, which is consistent with our hypothesis. We note, however, that this is a diagnostic result, and it does not indicate causality. Furthermore, another study found that moistening of the subsidence region of TCs with a long time scale results in a larger steady-state intensity than in a simulation with no moistening in an axisymmetric model (Rousseau-Rizzi et al., 2021), which seems to contradict our hypothesis. Other plausible explanations include that asymmetries in convection outside the eyewall may lead to the weakening of the TCs (David S. Nolan et al., 2007) or that the environmental maximum potential intensity of TCs is reduced by modification of the moisture field (Bister & Emanuel, 1998). However, computation of the potential intensity with the routine provided by Bister and Emanuel (Bister & Emanuel, 2002) does not support this hypothesis (see Figure S2 in the supplemental material). A conclusive investigation of the causes for the different intensities when weakening the MEC feedback on the “long” timescales would require a deeper study.

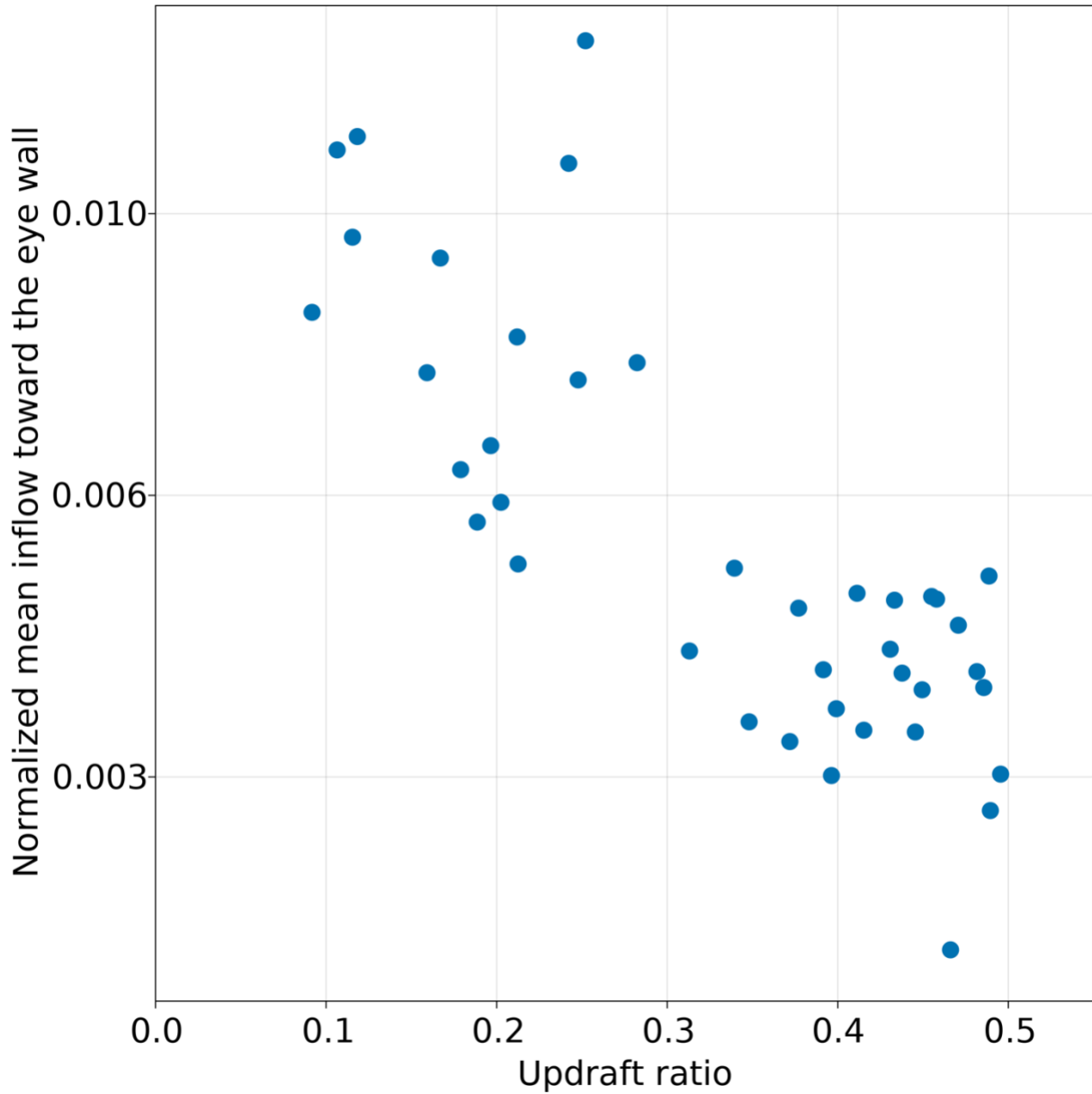


Figure 4. The absolute value of mean radial velocity from $r = 0$ to r_{max} from surface to $z = 6$ km, normalized by the maximum tangential wind speed vs. the updraft ratio. The vertical axis has a logarithmic scale.

5. Main findings and implications

This work answers what process is responsible for spontaneous TC genesis in the absence of radiative and surface-flux feedbacks in the simulations of Ramírez Reyes and Yang (2021). We perform mechanism-denial experiments using cloud-permitting simulations to test the hypothesis

that the MEC feedback is responsible for spontaneous TC genesis and intensification in the absence of radiative and surface-flux feedbacks. In the MEC feedback, moisture detrained from convective clouds moistens the environment and makes it favorable for new convective clouds, and drying by subsidence inhibits convection in the region. Both processes can lead to the convective organization (Tompkins, 2001). We find that the moisture gradients created by the MEC feedback lead to spontaneous TC genesis and intensification in the absence of radiative and surface-flux feedbacks.

The MEC feedback influences spontaneous TC genesis and intensification in two different time scales. Using dimensional analysis, we estimate that the entrainment and detrainment time scale is about a few hours, setting the short time scale of the MEC feedback. We test this prediction by weakening the MEC feedback across different time scales. We observe that using a time scale shorter than 2 hours, spontaneous TC genesis is inhibited, which corroborates our hypothesis. This “fast” time scale suggests that the MEC feedback is efficient and relevant for real-world TC genesis. For example, this result seems consistent with the real case study of Wang (2014), who pointed out that repeated congestus convection moistens the lower troposphere, leading to organized convection and to TC genesis.

Subsidence drying sets a time scale of ~ 17 days. We propose that subsidence drying promotes intensification of the TC by preventing the appearance of new convective events far from the radius of maximum winds, which would reduce the radial advection of angular momentum required for intensification of the TC (Montgomery & Smith, 2014). When we homogenize clear-sky water vapor on a multi-day time scale, we observe more frequent updrafts far from the eyewall of incipient TCs. This is accompanied by reduced inflow and lower TC intensity when compared with experiments with longer relaxation time scales or with no relaxation. This result again is consistent with our hypothesis. However, there are other possible explanations for the decreased TC intensity when using shorter water vapor-nudging timescale. For example, vertical wind shear (Alland et al., 2017), advection of dry environmental air (Wu et al., 2015), and moisture-radiation feedbacks (Ruppert et al., 2020) can all affect TC intensity. Examining these mechanisms in our modeling framework will require future research.

Data and software availability:

Following the Best Practices for Preservation and Replicability (Schuster et al., 2022), we make available the code and instructions to replicate our results. The system for atmospheric modeling (SAM) is free software and can be obtained from <http://rossby.msrc.sunysb.edu/~marat/SAM.html>. The version used in this work together with modified source code, initialization profiles, namelists and data analysis scripts are hosted on Zenodo and can be found with the digital object identifier (DOI) 10.5281/zenodo.6978839 (Ramírez Reyes & Yang, 2022). The data was analyzed using the Julia Programming Language (Bezanson et al., 2017) available under MIT license at www.julialang.org, with the Images.jl package available with MIT license at <https://github.com/JuliaImages/Images.jl>. Figures were created using the Makie.jl package (Danisch & Krumbiegel, 2021) available under MIT license at <https://github.com/JuliaPlots/Makie.jl>.

Acknowledgments

Argel Ramírez Reyes was supported by a CONACYT-UCMexus fellowship. Da Yang was supported by Laboratory Directed Research and Development (LDRD) funding from Berkeley Lab, provided by the Director, Office of Science, of the U.S. Department of Energy under Contract DE-AC0205CH11231, and the U.S. Department of Energy, Office of Science, Office of Biological and Environmental Research, Climate and Environmental Sciences Division, Regional and Global Climate Modeling Program under Award DE-AC0205CH11231. Da Yang was also supported by a Packard Fellowship for Science and Engineering, and the France-Berkeley Fund. Argel Ramírez Reyes thanks María Fernanda Ramírez Nazario for the creation of Figure 1, and Adrian Tompkins and Chis Davis for their useful input in the early stages of this work.

References

Alland, J. J., Tang, B. H., & Corbosiero, K. L. (2017). Effects of Midlevel Dry Air on Development of the Axisymmetric Tropical Cyclone Secondary Circulation. *Journal of the Atmospheric Sciences*, 74(5), 1455–1470. <https://doi.org/10.1175/JAS-D-16-0271.1>

- Bezanson, J., Edelman, A., Karpinski, S., & Shah, V. B. (2017). Julia: A Fresh Approach to Numerical Computing. *SIAM Review*, *59*(1), 65–98. <https://doi.org/10.1137/141000671>
- Bister, M., & Emanuel, K. A. (1998). Dissipative heating and hurricane intensity. *Meteorology and Atmospheric Physics*, *65*(3), 233–240. <https://doi.org/10.1007/BF01030791>
- Bister, M., & Emanuel, K. A. (2002). Low frequency variability of tropical cyclone potential intensity 1. Interannual to interdecadal variability. *Journal of Geophysical Research: Atmospheres*, *107*(D24), ACL 26-1-ACL 26-15. <https://doi.org/10.1029/2001JD000776>
- Bretherton, C. S., Blossey, P. N., & Khairoutdinov, M. F. (2005). An Energy-Balance Analysis of Deep Convective Self-Aggregation above Uniform SST. *Journal of the Atmospheric Sciences*, *62*(12), 4273–4292. <https://doi.org/10.1175/JAS3614.1>
- Bryan, G. H., Wyngaard, J. C., & Fritsch, J. M. (2003). Resolution Requirements for the Simulation of Deep Moist Convection. *Monthly Weather Review*, *131*(10), 2394–2416. [https://doi.org/10.1175/1520-0493\(2003\)131<2394:RRFTSO>2.0.CO;2](https://doi.org/10.1175/1520-0493(2003)131<2394:RRFTSO>2.0.CO;2)
- Carstens, J. D., & Wing, A. A. (2020). Tropical Cyclogenesis From Self-Aggregated Convection in Numerical Simulations of Rotating Radiative-Convective Equilibrium. *Journal of Advances in Modeling Earth Systems*, *12*(5), e2019MS002020. <https://doi.org/10.1029/2019MS002020>
- Chavas, D. R., Lin, N., & Emanuel, K. (2015). A Model for the Complete Radial Structure of the Tropical Cyclone Wind Field. Part I: Comparison with Observed Structure. *Journal of the Atmospheric Sciences*, *72*(9), 3647–3662. <https://doi.org/10.1175/JAS-D-15-0014.1>
- Collins, W., Rasch, P., Boville, B., McCaa, J., Williamson, D., Kiehl, J., et al. (2004). *Description of the NCAR Community Atmosphere Model (CAM 3.0)* [Application/pdf] (p. 12360 KB). UCAR/NCAR. <https://doi.org/10.5065/D63N21CH>
- Craig, G. C., & Mack, J. M. (2013). A coarsening model for self-organization of tropical convection. *Journal of Geophysical Research: Atmospheres*, *118*(16), 8761–8769. <https://doi.org/10.1002/jgrd.50674>
- Craig, George C., & Dörnbrack, A. (2008). Entrainment in Cumulus Clouds: What Resolution is Cloud-Resolving? *Journal of the Atmospheric Sciences*, *65*(12), 3978–3988. <https://doi.org/10.1175/2008JAS2613.1>
- Cronin, T. W., & Chavas, D. R. (2019). Dry and semi-dry tropical cyclones. *Journal of the Atmospheric Sciences*. <https://doi.org/10.1175/JAS-D-18-0357.1>

- Danisch, S., & Krumbiegel, J. (2021). Makie.jl: Flexible high-performance data visualization for Julia. *Journal of Open Source Software*, 6(65), 3349. <https://doi.org/10.21105/joss.03349>
- Davis, C. A. (2015). The Formation of Moist Vortices and Tropical Cyclones in Idealized Simulations. *Journal of the Atmospheric Sciences*, 72(9), 3499–3516. <https://doi.org/10.1175/JAS-D-15-0027.1>
- Deardorff, J. W. (1980). Stratocumulus-capped mixed layers derived from a three-dimensional model. *Boundary-Layer Meteorology*, 18(4), 495–527. <https://doi.org/10.1007/BF00119502>
- Grabowski, W. W., & Moncrieff, M. W. (2004). Moisture–convection feedback in the tropics. *Quarterly Journal of the Royal Meteorological Society*, 130(604), 3081–3104. <https://doi.org/10.1256/qj.03.135>
- Khairoutdinov, M. F., & Emanuel, K. A. (2013). Rotating radiative-convective equilibrium simulated by a cloud-resolving model. *Journal of Advances in Modeling Earth Systems*, 5(4), 816–825. <https://doi.org/10.1002/2013MS000253>
- Khairoutdinov, M. F., & Randall, D. A. (2003). Cloud Resolving Modeling of the ARM Summer 1997 IOP: Model Formulation, Results, Uncertainties, and Sensitivities. *Journal of the Atmospheric Sciences*, 60(4), 607–625. [https://doi.org/10.1175/1520-0469\(2003\)060<0607:CRMOTA>2.0.CO;2](https://doi.org/10.1175/1520-0469(2003)060<0607:CRMOTA>2.0.CO;2)
- Kiehl, T., Hack, J., Bonan, B., Boville, A., Briegleb, P., Williamson, L., & Rasch, J. (1996). Description of the NCAR Community Climate Model (CCM3). <https://doi.org/10.5065/D6FF3Q99>
- Kuang, Z., & Bretherton, C. S. (2006). A Mass-Flux Scheme View of a High-Resolution Simulation of a Transition from Shallow to Deep Cumulus Convection. *Journal of the Atmospheric Sciences*, 63(7), 1895–1909. <https://doi.org/10.1175/JAS3723.1>
- Lucas, C., Zipser, E. J., & Lemone, M. A. (1994). Vertical Velocity in Oceanic Convection off Tropical Australia. *Journal of the Atmospheric Sciences*, 51(21), 3183–3193. [https://doi.org/10.1175/1520-0469\(1994\)051<3183:VVIOCO>2.0.CO;2](https://doi.org/10.1175/1520-0469(1994)051<3183:VVIOCO>2.0.CO;2)
- Montgomery, M. T., & Smith, R. (2014). Paradigms for tropical cyclone intensification. *Australian Meteorological and Oceanographic Journal*, 64(1), 37–66. <https://doi.org/10.22499/2.6401.005>

- Muller, C. J., & Romps, D. M. (2018). Acceleration of tropical cyclogenesis by self-aggregation feedbacks. *Proceedings of the National Academy of Sciences*, *115*(12), 2930–2935. <https://doi.org/10.1073/pnas.1719967115>
- Nolan, David S., Moon, Y., & Stern, D. P. (2007). Tropical Cyclone Intensification from Asymmetric Convection: Energetics and Efficiency. *Journal of the Atmospheric Sciences*, *64*(10), 3377–3405. <https://doi.org/10.1175/JAS3988.1>
- Nolan, D.S. (2007). What is the trigger for tropical cyclogenesis? *Australian Meteorological Magazine*, *56*(4), 241–266.
- Ramírez Reyes, A., & Yang, D. (2021). Spontaneous Cyclogenesis without Radiative and Surface-Flux Feedbacks. *Journal of the Atmospheric Sciences*, *78*(12), 4169–4184. <https://doi.org/10.1175/JAS-D-21-0098.1>
- Ramírez Reyes, A., & Yang, D. (2022, August 10). The Moisture-Entrainment-Convection feedback can be sufficient to cause Spontaneous Tropical Cyclone Genesis. Zenodo. <https://doi.org/10.5281/zenodo.6978839>
- Randall, D. A., & Huffman, G. J. (1980). A Stochastic Model of Cumulus Clumping. *Journal of the Atmospheric Sciences*, *37*(9), 2068–2078. [https://doi.org/10.1175/1520-0469\(1980\)037<2068:ASMOCC>2.0.CO;2](https://doi.org/10.1175/1520-0469(1980)037<2068:ASMOCC>2.0.CO;2)
- Raymond, D. J., Sessions, S. L., & Fuchs, Ž. (2007). A theory for the spinup of tropical depressions. *Quarterly Journal of the Royal Meteorological Society*, *133*(628), 1743–1754. <https://doi.org/10.1002/qj.125>
- Romps, D. M. (2014). An Analytical Model for Tropical Relative Humidity. *Journal of Climate*, *27*(19), 7432–7449. <https://doi.org/10.1175/JCLI-D-14-00255.1>
- Rousseau-Rizzi, R., Rotunno, R., & Bryan, G. (2021). A Thermodynamic Perspective on Steady-State Tropical Cyclones. *Journal of the Atmospheric Sciences*, *78*(2), 583–593. <https://doi.org/10.1175/JAS-D-20-0140.1>
- Ruppert, J. H., Wing, A. A., Tang, X., & Duran, E. L. (2020). The critical role of cloud–infrared radiation feedback in tropical cyclone development. *Proceedings of the National Academy of Sciences*, 202013584. <https://doi.org/10.1073/pnas.2013584117>
- Schuster, D., Mayernik, M., & Mullendore, G. L. (2022). Products developed through the “What About Model Data?”, Determining Best Practices for Preservation and Replicability,

- EarthCube Research Coordination Network” project [Data set]. UCAR/NCAR - GDEX.
<https://doi.org/10.5065/G936-Q118>
- Scorer, R. S., & Ludlam, F. H. (1953). Bubble theory of penetrative convection. *Quarterly Journal of the Royal Meteorological Society*, 79(339), 94–103.
<https://doi.org/10.1002/qj.49707933908>
- Seeley, J. T., & Romps, D. M. (2015). Why does tropical convective available potential energy (CAPE) increase with warming? *Geophysical Research Letters*, 42(23), 10,429–10,437.
<https://doi.org/10.1002/2015GL066199>
- Seidel, S. D., & Yang, D. (2020). The lightness of water vapor helps to stabilize tropical climate. *Science Advances*, 6(19), eaba1951. <https://doi.org/10.1126/sciadv.aba1951>
- Tompkins, A. M. (2001). Organization of Tropical Convection in Low Vertical Wind Shears: The Role of Water Vapor. *Journal of the Atmospheric Sciences*, 58(6), 529–545.
[https://doi.org/10.1175/1520-0469\(2001\)058<0529:OOTCIL>2.0.CO;2](https://doi.org/10.1175/1520-0469(2001)058<0529:OOTCIL>2.0.CO;2)
- Tompkins, A. M., & Semie, A. G. (2017). Organization of tropical convection in low vertical wind shears: Role of updraft entrainment. *Journal of Advances in Modeling Earth Systems*, 9(2), 1046–1068. <https://doi.org/10.1002/2016MS000802>
- Wang, Z. (2012). Thermodynamic Aspects of Tropical Cyclone Formation. *Journal of the Atmospheric Sciences*, 69(8), 2433–2451. <https://doi.org/10.1175/JAS-D-11-0298.1>
- Wang, Z. (2014). Role of Cumulus Congestus in Tropical Cyclone Formation in a High-Resolution Numerical Model Simulation. *Journal of the Atmospheric Sciences*, 71(5), 1681–1700. <https://doi.org/10.1175/JAS-D-13-0257.1>
- Wing, A. A., Camargo, S. J., & Sobel, A. H. (2016). Role of Radiative–Convective Feedbacks in Spontaneous Tropical Cyclogenesis in Idealized Numerical Simulations. *Journal of the Atmospheric Sciences*, 73(7), 2633–2642. <https://doi.org/10.1175/JAS-D-15-0380.1>
- Wu, L., Su, H., Fovell, R. G., Dunkerton, T. J., Wang, Z., & Kahn, B. H. (2015). Impact of environmental moisture on tropical cyclone intensification. *Atmospheric Chemistry and Physics*, 15(24), 14041–14053. <https://doi.org/10.5194/acp-15-14041-2015>
- Yang, D. (2018). Boundary Layer Diabatic Processes, the Virtual Effect, and Convective Self-Aggregation. *Journal of Advances in Modeling Earth Systems*, 10(9), 2163–2176.
<https://doi.org/10.1029/2017MS001261>

Yang, D. (2019). Convective Heating Leads to Self-Aggregation by Generating Available Potential Energy. *Geophysical Research Letters*, 46(17–18), 10687–10696.
<https://doi.org/10.1029/2019GL083805>

Yang, D., & Seidel, S. D. (2020). The Incredible Lightness of Water Vapor. *Journal of Climate*, 33(7), 2841–2851. <https://doi.org/10.1175/JCLI-D-19-0260.1>